Characterization of Isomeric Structures in a Mixture of Organosilanes Using Multidimensional NMR

Weixia Liu and Peter L. Rinaldi*

Knight Chemical Laboratory, Department of Chemistry, The University of Akron, Akron, Ohio 44325-3601

Laurine Galya,† Joan E. Hansen,‡ and Lech Wilczek†

Corporate Research & Development, Dupont Experimental Station, Wilmington, Delaware 19880, and Dupont Automotive, Marshall Laboratory, 3401 Grays Ferry Avenue, Philadelphia, Pennsylvania 19146

Received March 4, 2002

Triple resonance $^{1}H/^{13}C/^{29}Si$ three-dimensional nuclear magnetic resonance methods were used to characterize the isomeric structures in a mixture of isomeric disilylated 4-vinyl-1-cyclohexene. Triple resonance techniques when used together with pulsed field gradient coherence selection permit selective detection of the structure fragments of $^{1}H-^{13}C-^{29}Si$ spin systems. Three-frequency correlation provides a method of separating the resonances from a complex mixture of isomers without physical separation of the components. Many signals that are not resolvable in 1D NMR or 2D NMR spectra can be seen with the aid of triple resonance 3D NMR techniques. The experiment was done in three ways to selectively detect correlations between ^{29}Si resonances and CH_n groups which are one, two, and three bonds away. The combined data from the three experiments provide unambiguous atomic connectivity information.

Introduction

Reactive silanes have found broad use as curing and coupling agents in adhesives, sealants, and coatings.[1] The development of novel coating technologies is strongly driven by environmental legislation to reduce the volatile organic content (VOC) released into the atmosphere during cure of the film. The use of silane-based reactive diluents to produce high solids coatings is an attractive way to respond to this drive. These low molecular weight silanes play an analogous role to solvents used in high VOC formulations in that they reduce viscosity. However, these diluents become incorporated into the film upon curing and thus do not contribute to VOC. This paper describes the detailed NMR characterization of the various isomers formed in synthesizing these multifunctional silane diluents according to eq 1. Since the distribution of isomers is an important determinant of reactivity, detailed structure analysis is necessary in order to optimize the synthesis of the diluents as well as the final coating formulation.[2]

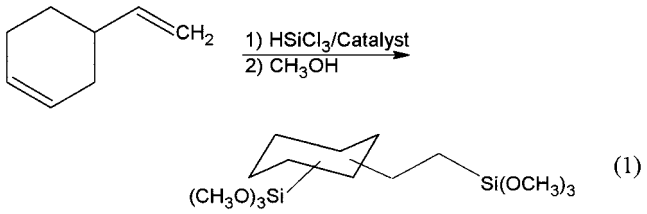

(1)

High-resolution NMR has been one of the most powerful tools for determining the structures of organic molecules in solution. However, when tackling the structures of complex molecules or mixtures of simple molecules, which are the targets of many modern synthetic efforts, even one-dimensional (1D) and two-dimensional (2D) NMR techniques at high field may not yield unambiguous answers. This is because of extensive overlap in critical regions of the spectra. Three-dimensional (3D), triple resonance NMR techniques have been extremely useful for the structural elucidation of biological macromolecules over the past decade.[3] Only recently have researchers begun using these methods to study organic structures.

Most 3D NMR experiments use ^{1}H detection and rely on multiple step magnetization transfers via resolved *J*-couplings between three nuclei H, X, and Y.[4] The higher spectral dispersion is obtained by correlating the chemical shifts of two or three different types of NMR active nuclei along three chemical shift axes. The presence of peaks correlating the chemical shifts of these three nuclei establish atomic connectivity relationships which are determined by the *J*-couplings present in the molecule and the delays used in the experiment.

* Corresponding author. Tel: 330-972-5990. Fax: 330-972-5256. E-mail: PeterRinaldi@uakron.edu.
† Corporate Research & Development, Dupont Experimental Station.
‡ Dupont Automotive.

(1) Gregorovich, B. V. *Paint Coatings Ind.* **1998**, *June*, 76.
(2) Adamsons, K.; Blackman, G.; Gregorovich, B.; Lin, L.; Matheson, R. *Prog. Org. Coat.* **1998**, *34*, 64.
(3) (a) Ikura, M.; Kay, L. E.; Bax, A. *Biochemistry* **1990**, *29*, 4659. (b) Kay, L. E.; Ikura, M.; Tschudin, R.; Bax, A. *J. Magn. Reson.* **1990**, *89*, 496. (c) Bax, A.; Grzesiek, S. *Acc. Chem. Res.* **1993**, *26*, 131. (d) Cavanagh, J.; Fairbrother, W. J.; Palmer, G. A., III; Skelton, N. J. *Protein NMR Spectroscopy Principles and Practice*; Academic Press: New York, 1996; Chapter 8.
(4) Whitehead, B.; Craven, C. J.; Waltho, J. P. In *Protein NMR Techniques*; Reid, D. G., Ed.; Humana Press: Totowa, NJ, 1997; p 29.

10.1021/om020177x CCC: $22.00
Publication on Web 06/12/2002

Biological applications of triple resonance 3D NMR have mostly relied on the use of ^{13}C and ^{15}N labeling to enhance the abundance of $^{1}H-^{13}C-^{15}N$ spin systems, which produce the correlations observed. Most applications of triple resonance 3D NMR methods in the study of synthetic organic molecules have taken advantage of the high natural abundance of at least two of the nuclei involved in the experiment. Typically, ^{1}H is the first nucleus, ^{31}P or ^{19}F (both 100% natural abundance) would be the X nucleus, and ^{13}C would be the Y nucleus. One particularly interesting application[5] involves determination of the isomeric structures in mixtures, which are not physically separated, but whose spectra can be separated on the basis of the signals in multidimensional NMR experiments. This approach has been used to determine the structures present in mixtures using $^{1}H/^{13}C/^{19}F$,[6] $^{1}H/^{13}C/^{31}P$,[7] and $^{1}H/^{13}C/^{29}Si$[8] triple resonance 3D NMR experiments without resorting to isotopic labeling. This paper demonstrates that $^{1}H/^{13}C/^{29}Si$ triple resonance 3D NMR techniques at natural abundance can provide a useful method for separating signal components of a mixture without preseparation of the components in the sample mixture.

Experimental Section

Synthesis of (2-Trimethoxysilyl)ethyl(trimethoxysilyl)-cyclohexane. To a 350 mL pressure glass reactor was added 4-vinyl-1-cyclohexene (15 g, 0.138 mol), trichlorosilane (60 g, 0.443 mol), and platinum-divinyltetramethylsiloxane complex (2−3 wt % platinum in xylenes, #PC072 from United Chemical Technologies).[9] The reactor was tightly closed and heated at 115 °C for 4 h. The excess trichlorosilane was stripped under high vacuum. A gas chromatography analysis showed the desired disilylated product in 43% yield, the remaining components in the reaction mixture being the corresponding monosilylated intermediate. A mixture of anhydrous methanol (20 g, 0.625 mol) and trimethylorthoformate (90 g, 0.85 mol) was added dropwise to the reaction mixture, with stirring, under slight vacuum, and at a rate to keep the internal temperature below 30 °C. After the addition was complete, triethylamine (2.5 g, 0.025 mol) was added and the mixture was refluxed for 2 h. The volatiles were distilled from the mixture. The reaction mixture was then distilled at 80−110 °C under a vacuum of 0.03−0.1 Torr, collecting ca. 70% forecut and several fractions using a Kugelrohr apparatus. Gas chromatography, mass spectrometry, and NMR analysis indicated the desired structures were present in the later fractions in >95% purity, 10 g (30% yield), colorless liquid, viscosity <0.1 P at 25 °C. The disilylated adduct was composed of several regio- and stereoisomers as characterized by NMR.

General NMR. NMR spectra were obtained using a Varian VXR 300 MHz spectrometer with a 10 mm broadband probe and a Varian Unityplus 600 MHz NMR spectrometer equipped with three broadband RF channels, Performa 1 pulsed field gradient accessory, and a Nalorac $^{1}H/^{13}C/X/^{2}H$ (where X is tunable over the range of resonance frequencies from ^{31}P to ^{15}N) four-channel probe equipped with a *z*-axis pulsed field gradient coil. Spectra were obtained from ca. 200 mg of the isomer mixture in 0.7 mL of $CDCl_3$ unless otherwise mentioned. All NMR data were processed with Varian's VNMR software on a Sun workstation. $CDCl_3$ was used as an internal reference for the ^{1}H chemical shifts ($\delta_{^{1}H} = 7.24$), and TMS was used as an external reference for ^{29}Si chemical shift and ^{13}C chemical shift ($\delta_{^{29}Si} = 0$, $\delta_{^{13}C} = 0$).

Acquisition of 1D ^{29}Si NMR Spectrum. The 59.6 MHz 1D ^{29}Si spectrum was obtained with a VXR-300 spectrometer using the following parameters: a 1.4 s acquisition time, 30 kHz spectral window, 12.5 μs (90°) pulse, 12 s relaxation delay, WALTZ-16 modulated gated decoupling (2.2 kHz decoupling field, during the acquisition time only), and averaging of 64 transients. The data were processed by zero filling to 128K and exponentially weighting with a 1 Hz line-broadening before Fourier transformation.

Acquisition of 2D ^{1}H−^{13}C and ^{1}H−^{29}Si HMQC NMR Spectra. The $^{1}H-^{13}C$ HMQC NMR spectrum was obtained with the States method[10] of phase-sensitive detection, using 90° pulses for ^{1}H and ^{13}C of 10.7 and 21.0 μs, respectively, a relaxation delay of 1.0 s, a delay Δ of 1.79 ms (based on $^{1}J_{CH} = 140$ Hz), and a 0.049 acquisition time (with GARP1-modulated ^{13}C decoupling[11]). Eight transients were averaged for each of 512 increments during t_1, and 256 points were collected during t_2. The evolution times were incremented to provide the equivalent of a 10015.6 Hz spectral window in the f_1 dimension, and a 2686.0 Hz spectral window was used in the f_2 dimension. The total experiment time was ca. 2 h. The data were zero-filled to 2048 × 1024 points and weighted with a Gaussian function before Fourier transformation.

The following parameters were used in the $^{1}H-^{29}Si$ PFG-HMQC experiment: ^{1}H and ^{29}Si 90° pulse widths of 10.7 and 13.0 μs, respectively; 2686.0 and 1548.1 Hz spectral windows in the ^{1}H (f_2) and ^{29}Si (f_1) dimensions, respectively; a relaxation delay of 1.0 s, a delay $\Delta = 27.8$ ms (optimized for $1/(4 \times {}^{2}J_{HSi})$), and a 0.05 s acquisition time with ^{29}Si MPF6 decoupling.[12] Eight transients were averaged for each of 512 increments during t_1, and 256 points were sampled during t_2. The strengths of the three 2.0 ms PFG's were $g_1 = 0.300$, $g_2 = 0.300$, and $g_3 = -0.119$ T m^{-1}. The data were processed with a shifted sinebell weighting, and the spectrum was displayed in the magnitude-mode in both dimensions. 2D Fourier transformation was performed on a 1024 × 512 matrix.

Acquisition of 3D ^{1}H/^{13}C/^{29}Si NMR Spectra. The 3D $^{1}H/^{13}C/^{29}Si$ NMR spectra were obtained with the States method to provide phase-sensitive detection in all three dimensions, using 90° pulses for ^{1}H, ^{13}C, and ^{29}Si of 10.7, 21.0, and 13.0 μs, respectively, a relaxation delay of 1.0 s, a delay Δ of 1.79 ms (based on $^{1}J_{CH} = 140$ Hz), and a 0.048 s acquisition time (with simultaneous ^{29}Si and ^{13}C MPF20 decoupling); four transients were averaged for each of 2 × 64 increments during t_1, 2 × 24 increments during t_2, and 256 points in t_3. Three separate experiments were performed once each with $\tau = 2.60$, 19.2, and 50.0 ms (based on $^{1}J_{CSi} = 96$ Hz, $^{n}J_{CSi} = 13$ Hz, and $^{n}J_{CSi} = 5$ Hz). The evolution times were incremented to provide the equivalent of 8847.6 and 1548.1 Hz spectral windows in the f_1 and f_2 dimensions, respectively, and a 2636.6 Hz spectral window in the f_3 dimension. The field gradient pulses had durations of 1.0 ms and amplitudes of 0.3 and 0.0601 T/m for the first and second pulses, respectively (set based on the ratio of the ^{1}H and ^{29}Si resonance frequencies). The total experiment time was ca. 6 h. The data were zero filled to 256 × 128 ×

(5) (a) Parker, D. *Chem. Rev.* **1991**, *91*, 1441. (b) Tokles, M.; Keifer, P. A.; Rinaldi, P. L. *Macromolecules* **1995**, *28*, 3944.
(6) (a) Li, L.; Ray, D. G., III; Rinaldi, P. L.; Wang, H.-T.; Harwood, H. J. *Macromolecules* **1996**, *29*, 4706. (b) Li, L.; Rinaldi, P. L. *Macromolecules* **1996**, *29*, 4808.
(7) (a) Berger, S.; Bast, P. *Magn. Reson. Chem.* **1993**, *31* (11), 1021. (b) Saito, T.; Rinaldi, P. L. *J. Magn. Reson.* **1996**, *118*, 136. (c) Saito, T.; Rinaldi, P. L. *J. Magn. Reson.* **1998**, *130*, 135.
(8) Chai, M.; Saito, T.; Pi, Z.; Tessier, C.; Rinaldi, P. L. *Macromolecules* **1997**, *30*, 1240.
(9) Spier, J. L. In *Advances in Organometllic Chemistry Catalysis and Organic Syntheses*; West, R., Stone, F. G. A., Eds.; Academic Press: New York, 1979; Vol. 17, p 407.
(10) States, D. J.; Haberkorn, R. A.; Ruben, D. J. *J. Magn. Reson.* **1982**, *48*, 286.
(11) Shaka, A. J.; Barker, P. B.; Freeman, R. *J. Magn. Reson.* **1985**, *64*, 547.
(12) (a) Fujiwara, T.; Nagayama, K. *J. Magn. Reson.* **1988**, *77*, 53. (b) Fujiwara, T.; Anai, T.; Kurihara, N.; Nagayama, K. *J. Magn. Reson.* **1993**, *104*, 103.

Scheme 1. Synthesis and Structures of Hydrosilylated Products of 4-Vinyl-1-cyclohexene

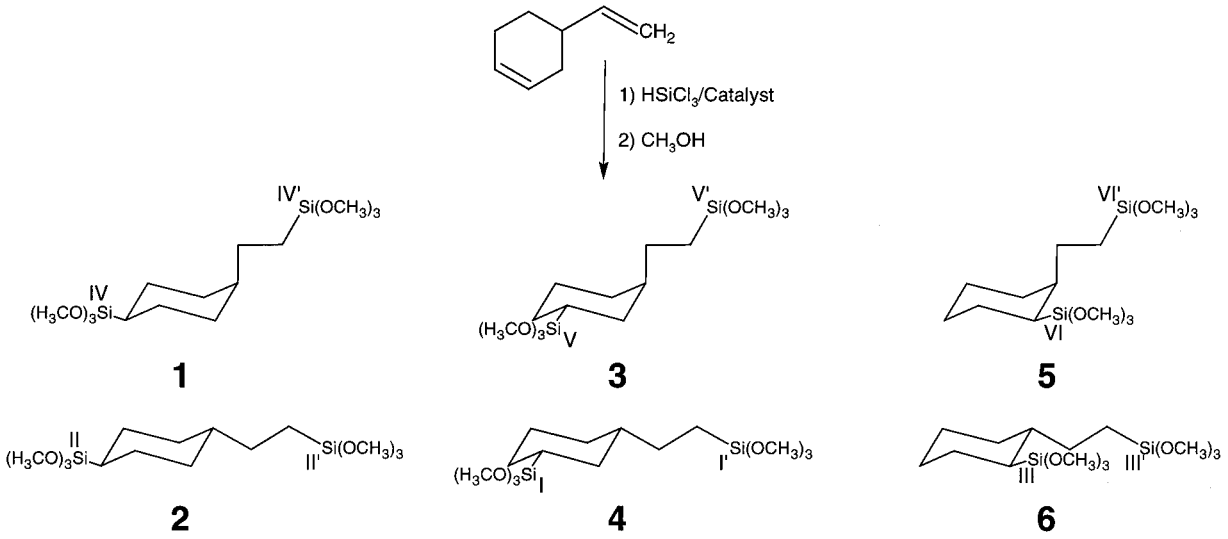

1024 complex points and weighted with a shifted Gaussian function before Fourier transformation.

Result and Discussion

Preparation and Structure of Hydrosilylated Products from 4-Vinyl-1-cyclohexene. This study focuses on the NMR characterization of six (2-trimethoxysilyl)ethyl(trimethoxysilyl)cyclohexane isomers prepared with Pt catalyst (ds-4-VCH/Pt). The synthesis of the sample of ds-4VCH/Pt isomers is outlined in Scheme 1. Hydrosilylation of 4-vinyl-1-cyclohexene was accomplished with $HSiCl_3$ in the presence of a platinum catalyst. Methoxylation was accomplished by refluxing with methanol and trimethylorthoformate. The ds-4VCH/Pt product contained six stereoisomers as shown in Scheme 1.

The hydrosilylation of a diene having a low reactivity internal double bond and catalyzed by a transition metal yields a complex mixture of regio- and stereoisomers. Internal double bond isomerization/migration may also occur, adding to the complexity of this reaction. In contrast, hydrosilylation using the same substrates but initiated by radicals was more effective, giving higher reactivity and product selectivity as described in U.S. Patents 5,527,936[13] and 5,530,152.[14]

The synthesis of alkoxysilanes by hydrosilylation of a low reactivity internal double bond is usually a two-step process.[15] Chlorohydrosilanes, which are more reactive than the corresponding alkoxyhydrosilanes, are required for the first step of the reaction involving slow hydrosilylation. The desired alkoxysilanes are obtained in the second step of the process, which involves fast alkoxylation of the chlorosilylated intermediate.

1D and 2D NMR Spectra

Figure 1 shows expansions from the ^1H, ^{13}C, and ^{29}Si 1D NMR spectra of disilylated 4-vinyl-1-cyclohexene. In the ^1H 1D NMR spectrum, similar methylene and methine resonances all overlap. The ^{29}Si 1D NMR spectrum shows two groups of resonances. Each group has six types of Si species, one from each of the six isomers present in the hydrosilylated products of 4-vinyl-1-cyclohexene. The signals in the range −41.0 to −41.4 ppm come from the $-Si(OMe)_3$ groups bound to the ethyl side chain. The signals in the range −44.5 to −46.0 ppm come from the $-Si(OMe)_3$ groups bound to the cyclohexyl ring. The six pairs of silicon resonances, which are attributed to six isomers in the mixture, can be matched on the basis of their relative intensities in

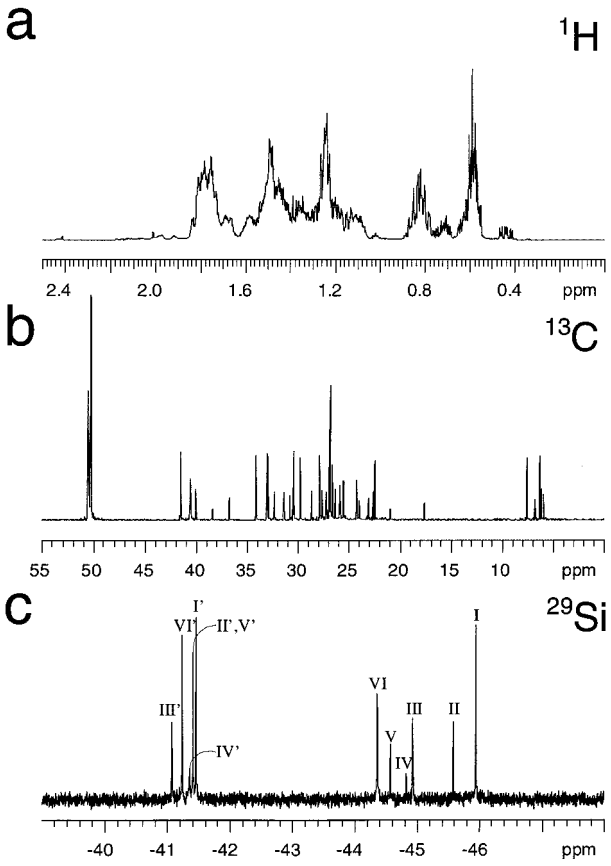

Figure 1. 1D NMR spectra of disilylated 4-vinyl-1-cyclohexene in $CDCl_3$ collected at 30 °C: (a) expansion of the methylene region from 600 MHz ^1H spectrum; (b) 150 MHz ^{13}C spectrum with ^1H decoupling; (c) 59.59 MHz ^{29}Si spectrum.

(13) Dindi, H.; Gregorovich, B.; Hazan, I.; Mulligan, S. US Patent 5527936, 1996.
(14) Dindi, H.; Mulligan, S. US Patent 5530152, 1996.
(15) Marciniec, B.; et al. *Comprehensive Handbook on Hydrosilylation*; Pergamon Press: Oxford, 1992; pp 35−153

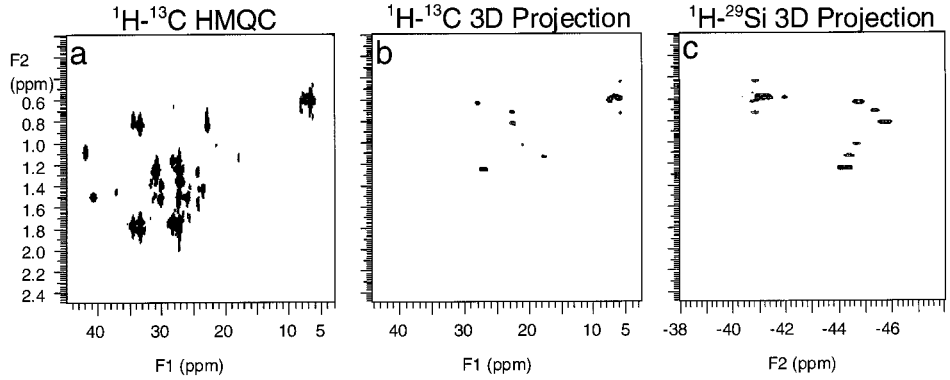

Figure 2. 2D NMR spectra and projections of the 3D NMR spectrum of disilylated 4-vinyl-1-cyclohexene in $CDCl_3$: (a) ^{1}H−^{13}C HMQC 2D NMR spectrum; (b) ^{1}H−^{13}C (f_1f_3) projection of the ^{1}H/^{13}C/^{29}Si 3D NMR spectrum; (c) ^{1}H−^{29}Si (f_2f_3) projection of the ^{1}H/^{13}C/^{29}Si 3D NMR spectrum. The total experiment time for the 3D NMR spectrum was ca. 6 h.

this spectrum from the six-isomer mixture, and a second spectrum (not shown) from a four-isomer mixture (containing only ^{29}Si resonances I/I′, II/II′ IV/IV′, and V/V′). Therefore, assignments of the latter −Si(OMe)$_3$ resonances (discussed below) provide the assignments of the former −Si(OMe)$_3$ resonances. Because of the overlap in the 1D proton spectra and the slight difference in carbon chemical shift, it is still quite difficult to distinguish and assign resonances in these spectra.

Figure 2a shows a plot of the expansion from the standard ^{1}H−^{13}C heteronuclear multiple quantum coherence (HMQC)[16] 2D NMR spectrum of disilylated 4-vinyl-1-cyclohexene. The spectrum shows the C−H correlations of all the isomers. There are so many similar cross-peaks that it is still not possible to distinguish all of the resonances, even in a 600 MHz 2D NMR spectrum. To resolve additional resonances, it is possible to disperse the resonances into a third dimension on the basis of the chemical shifts of a third type of nucleus (^{29}Si in this case).

3D NMR Pulse Sequence. Figure 3 shows the pulse sequence used to collect the ^{1}H/^{13}C/^{29}Si chemical shift correlation 3D NMR spectra. It is a modified version of the HNCA pulse sequence used in conjunction with ^{13}C and ^{15}N isotopic labeling to assign the backbone resonances of proteins.[17] The experiment uses $^1J_{CH}$ and $^nJ_{CSi}$ to sequentially transfer NMR coherence along the path ^{1}H→^{13}C→^{29}Si→^{13}C→^{1}H, as illustrated by the arrows in the structure in Figure 3. The Δ and τ delays are set to $1/(4 \times {}^1J_{CH})$ and $1/(4 \times {}^nJ_{CSi})$, respectively. Evolution times are inserted where the coherence resides on ^{29}Si and ^{13}C, to encode the chemical shifts of these nuclei in the indirectly detected dimensions. The gradient area ratios ($g_1/g_2 = \nu_H/\nu_{Si}$) are set to selectively refocus and detect signals originating from 0.05% of the molecules containing the ^{1}H−^{13}C−^{29}Si spin systems [0.011 (abundance of ^{13}C) × 0.048 (abundance of ^{29}Si)]. The experiment is made more difficult by the fact that there are at least six possible structures in the mixture. Detection is therefore limited by the amount of the least concentrated isomer, which is ca. 5% of the mixture on the basis of the integrals in the 1D ^{29}Si spectrum. If all these

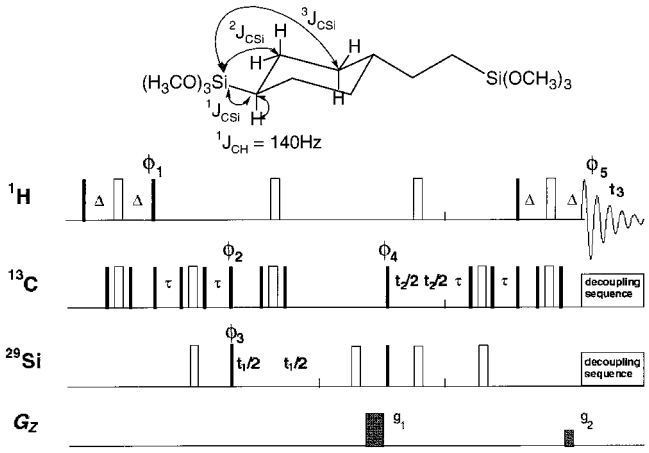

Figure 3. Diagram of the pulse sequence used for the ^{1}H/^{13}C/^{29}Si 3D NMR experiment. Solid and unfilled pulses represent 90° and 180° flips with the following phases: $\phi_1 = \phi_2 = y$; $\phi_3 = x, -x$; $\phi_4 = y, y, -y, -y$; $\phi_5 = x, -x, -x, x$. Two data sets were obtained with different signs for the first PFG and combined to obtain a pure absorption mode spectrum in f_1.[24] ϕ_4 is incremented according to the States method during t_2, to provide a hypercomplex phase-sensitive 3D data set. Pulsed field gradients g_1 and g_2 are used to destroy undesired NMR signal components.

factors are considered, one realizes that successful completion of the experiment requires detection of signals having a relative intensity of 1 (from the ^{1}H−^{13}C−^{29}Si spin systems in the least concentrated structure), while uniformly and completely suppressing the signals of intensity 30,000 from the remainder of the protons in the sample! While this is a considerable challenge, with the aid of pulsed field gradients,[18] the stability of modern NMR instruments and a high sample concentration, it is possible.

Heteronuclear spin−spin coupling constants can be used to provide valuable information concerning the structure of molecules. The range for the splitting of satellites in a ^{29}Si spectrum due to the presence of ^{13}C one bond away is 37−113 Hz, and the range of two-bond coupling constants ($^2J_{CSi}$) is 0−18 Hz.[19] Individual values of $^3J_{CSi}$ have been reported that fall in the range

(16) (a) Muller, L. *J. Am. Chem. Soc.* **1979**, *101*, 4481. (b) Bax, A.; Griffey, R. H.; Hawkins, B. L. *J. Magn. Reson.* **1983**, *55*, 301.

(17) (a) Ikura, M.; Kay, L. E.; Bax, A. *Biochemistry* **1990**, *29*, 4659. (b) Kay, L. E.; Ikura, M.; Tschudin, R.; Bax, A. *J. Magn. Reson.* **1990**, *89*, 496. (c) Clore, G. M.; Bax, A.; Driscoll, P. C.; Wingfield, P. T.; Gronenborn, A. M. *Biochemistry* **1990**, *29*, 8172.

(18) (a) Hurd, R. E. *J. Magn. Reson.* **1990**, *87*, 422. (b) Rinaldi, P. L.; Keifer, P. A. *J. Magn. Reson.* **1994**, *108*, 259. (c) Rinaldi, P. L.; Ray, D. G., III; Litman, V. E.; Keifer, P. A. *Polym. Int.* **1995**, *36*, 177.

(19) Marsmann, H. C. In *Encyclopedia of Nuclear Magnetic Resonance*; Grant, D. M., Harris, R. K., Eds.; John Wiley & Sons: New York, 1996; Vol. 7, p 4386.

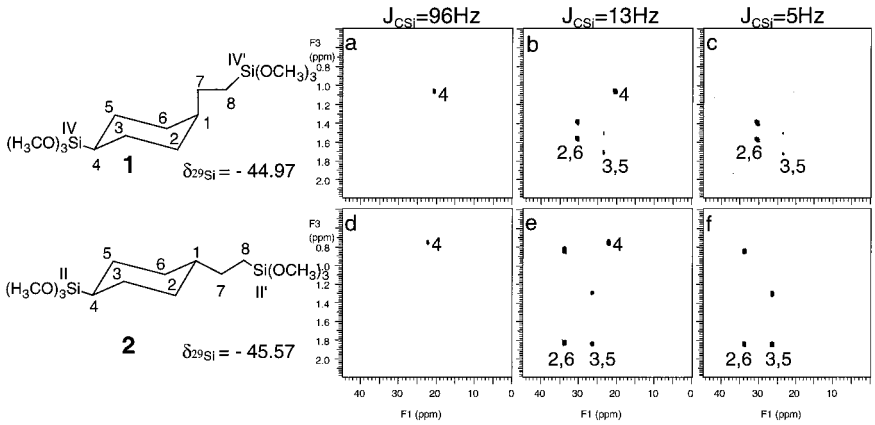

Figure 4. Slices, containing resonances of **1** and **2**, from the $^1H/^{13}C/^{29}Si$ 3D NMR spectrum of disilylated 4-vinyl-1-cyclohexene in $CDCl_3$: (a−c) and (d−f) are slices corresponding to $\delta_{^{29}Si} = -44.97$ and $\delta_{^{29}Si} = -45.57$, respectively; (a and d) are from the spectrum obtained with $\tau = 2.60$ ms (based on $^1J_{CSi} = 96$ Hz); (b and e) are from the spectrum obtained with $\tau = 19.2$ ms (based on $^nJ_{CSi} = 13$ Hz); (c and f) are from the spectrum obtained with $\tau = 50.0$ ms (based on $^nJ_{CSi} = 5$ Hz).

2−10 Hz.[20] Aliphatic trialkoxysilanes exhibit $^2J_{Csi}$ couplings in the range 2−5 Hz and $^3J_{Csi}$ couplings in the range 4−10 Hz, with the typically observed Karplus dependence of vicinal couplings on dihedral angle. Small molecules have reasonably long relaxation times, so experiments are feasible even with the long τ delays needed to transfer magnetization using these small, long-range coupling constants. This makes it possible to perform the 3D $^1H-^{13}C-^{29}Si$ experiment in one of three ways to obtain different structural information. If a spectrum is collected with $\tau = 1/(4 \times {}^1J_{CSi}) = 2.60$ ms ($^1J_{CSi} = 96$ Hz), slices at each of the ^{29}Si shifts will contain C−H chemical shift correlations for CH_n groups directly bound to ^{29}Si. If a spectrum is collected with $\tau = 1/(4 \times {}^nJ_{CSi}) = 19.2$ ms ($^nJ_{CSi} = 13$ Hz), then slices at each of these ^{29}Si shifts will primarily contain C−H correlations for CH_n groups three bonds away from ^{29}Si. If a spectrum is collected with $\tau = 1/(4 \times {}^nJ_{CSi}) = 50.0$ ms ($^nJ_{CSi} = 5$ Hz), then slices at each of the ^{29}Si shifts will contain more intense C−H correlations for CH_n groups two bonds away from ^{29}Si, compared with the intensities of these same cross-peaks observed in the spectrum collected with $\tau = 1/(4 \times {}^nJ_{CSi}) = 19.2$ ms.[21] Combined data from three experiments provide information about Si−C−H, Si−C−C−H, Si−C−C−C−H fragments, to identify the bonding pattern in the molecule and resolve all the resonances of ^1H, ^{13}C, and ^{29}Si.[22]

3D NMR Spectra. Figure 2b shows a projection of the $^1H/^{13}C/^{29}Si$ 3D NMR spectrum of disilylated 4-vinyl-1-cyclohexene onto the f_1f_3 plane ($^{13}C-^1H$ correlations). This spectrum was obtained with the τ delays optimized for one-bond C−Si couplings. In the $^1H/^{13}C/^{29}Si$ 3D NMR projection, only the correlations between resonances of protons and carbons of CH_n groups bound to ^{29}Si atoms are detected. The remainder of the signals, from nuclei that are not part of $^1H-^{13}C-^{29}Si$ spin systems, are removed from the spectrum. Six cross-peaks in the 15−30 ppm region are seen in the f_1f_3 projection of the $^1H/^{13}C/^{29}Si$ 3D NMR spectrum. These cross-peaks represent methine groups in the cyclohexyl ring which are bound to ^{29}Si. There are quite different proton and carbon chemical shifts because of the different ring positions of the attached $-Si(OMe)_3$ groups. But in the 6−8 ppm region, the cross-peaks show similar proton and carbon chemical shifts, which correspond to the $-Si(OMe)_3$ groups at the ends of the ethyl branches. This projection is much like the one obtained from the HMQC experiment; however, many of CH_n groups are filtered from the spectrum. As a result, Figure 2b is much simpler than the HMQC spectrum shown in Figure 2a.

Figure 2c shows a plot of the 3D projection of the $^1H/^{13}C/^{29}Si$ spectrum from disilylated 4-vinyl-1-cyclohexene onto the f_2f_3 plane ($^1H-^{29}Si$ correlations). Six major Si species are detected in this isomeric mixture, having ^{29}Si chemical shifts in the f_2 dimension of Si_I (−45.94 ppm), Si_{II} (−45.57 ppm), Si_{III} (−45.00 ppm), Si_{IV} (−44.97 ppm), Si_V (−44.69 ppm), and Si_{VI} (−44.65 ppm), corresponding to the peaks seen in the ^{29}Si 1D NMR spectrum. These represent the six different isomeric structures shown in Scheme 1.

Figures 4−6 show f_1f_3 slices (δ^1_H vs δ^{13}_C), at six different silicon chemical shifts, from the $^1H/^{13}C/^{29}Si$ 3D NMR spectra. These slices were taken from three separate 3D NMR spectra, obtained from the experiments using τ delays of 2.60, 19.2, and 50.0 ms. The slices shown in these figures are arranged in columns based on the τ delays used to acquire the spectra and are arranged in rows based on the ^{29}Si chemical shifts of each isomer. Each slice shows δ^1_H vs δ^{13}_C (f_1f_3) correlations of CH_n groups bound to the ^{29}Si atom having a chemical shift corresponding to the position of that slice in the f_2 dimension. The structures are determined by comparing the C−H correlations in slices

(20) Kupce, E.; Lukevics, E. In *Isotopes in the Physical and Biomedical Sciences*; Buncel, E., Jones, J. R., Eds.; Elsevier Science Publishers: Amsterdam, 1991; 2, Chapter 5, p 213.

(21) The cross-peak intensities in multidimensional NMR experiments are dependent on $\sin(2\pi \times \tau \times J)$. Ideally, a maximum intensity should be observed when $\tau = 1/4J$; however, the intensities are also attenuated by relaxation. Therefore, it is common practice to use τ delays somewhat smaller (based on a larger J coupling) than the optimum predicted based on the J coupling alone. In the experiment with delays based on $^nJ_{CSi} = 13$ Hz only about 30% attenuation is expected for correlations derived from interactions where $J_{CSi} = 6.5$ Hz (middle of the expected range for $^3J_{CSi}$); this signal loss is offset by the fact that signal losses due to relaxation effects during the long train of pulses is reduced. Only 1/3 of the theoretical maximum signal intensities is expected for correlations derived from interactions where $^nJ_{CSi} = 3$ Hz (middle of the expected range for $^2J_{CSi}$) in the experiment performed with delays optimized for $^nJ_{CSi} = 13$ Hz.

(22) Liu, W.; Saito, T.; Li, L.; Rinaldi, P. L.; Hirst, R.; Halasa, A. F.; Visintainer, J. *Macromolecules* **2000**, *33*, 2364.

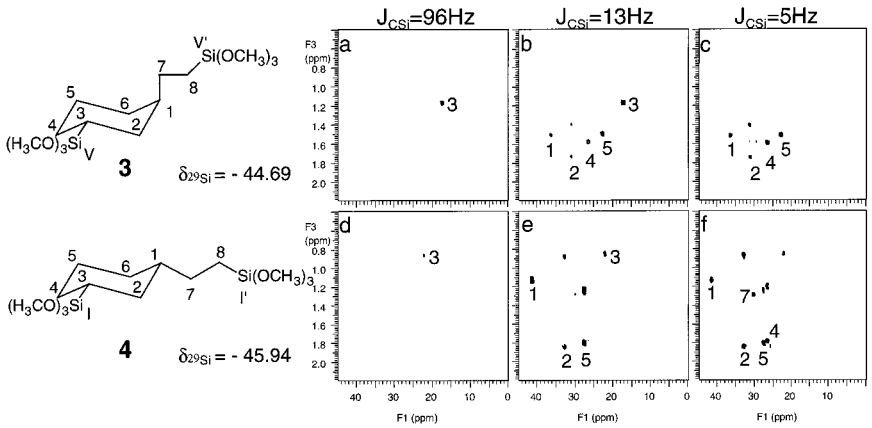

Figure 5. Slices, containing resonances of **3** and **4**, from the $^{1}H/^{13}C/^{29}Si$ 3D NMR spectrum of disilylated 4-vinyl-1-cyclohexene in $CDCl_3$: (a−c) and (d−f) are slices corresponding to $\delta_{^{29}Si} = -44.69$ and $\delta_{^{29}Si} = -45.94$, respectively; (a and d) are from the spectrum obtained with $\tau = 2.60$ ms (based on $^{1}J_{CSi} = 96$ Hz); (b and e) are from the spectrum obtained with $\tau = 19.2$ ms (based on $^{n}J_{CSi} = 13$ Hz); (c and f) are from the spectrum obtained with $\tau = 50.0$ ms (based on $^{n}J_{CSi} = 5$ Hz).

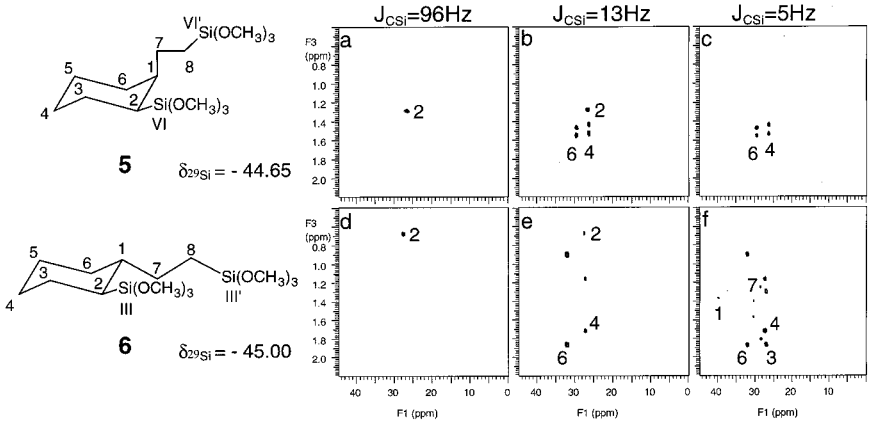

Figure 6. Slices, containing resonances of **5** and **6**, from the from $^{1}H/^{13}C/^{29}Si$ 3D NMR spectrum of disilylated 4-vinyl-1-cyclohexene in $CDCl_3$: (a−c) and (d−f) are slices corresponding to $\delta_{^{29}Si} = -44.65$ and $\delta_{^{29}Si} = -45.00$, respectively; (a and d) are from the spectrum obtained with $\tau = 2.60$ ms (based on $^{1}J_{CSi} = 96$ Hz); (b and e) are from the spectrum obtained with $\tau = 19.2$ ms (based on $^{n}J_{CSi} = 13$ Hz); (c and f) are from the spectrum obtained with $\tau = 50.0$ ms (based on $^{n}J_{CSi} = 5$ Hz).

at a specific ^{29}Si chemical shift, from the series of spectra. The slices in the columns labeled with $^{1}J_{CSi} =$ 96 Hz contain C−H correlations from only those CH_n groups directly bound to the ^{29}Si. The slices in the columns labeled with $^{n}J_{CSi} = 13$ Hz and $^{n}J_{CSi} = 5$ Hz contain C−H correlations primarily from those CH_n groups three and two bonds from ^{29}Si, respectively. However these slices also contain correlations from CH_n groups directly bound to the ^{29}Si. The latter correlations can easily be identified by comparison with the spectra in the first column ($^{1}J_{CSi} = 96$ Hz). Differentiation between C−H correlations from CH_n groups two and three bonds from ^{29}Si can be made by comparing the cross-peak intensities in the slices from the $^{n}J_{CSi} = 13$ Hz and $^{n}J_{CSi} = 5$ Hz spectra. The cross-peaks from the three-bond correlations will be more intense in the $^{n}J_{CSi} = 13$ Hz spectrum than in the $^{n}J_{CSi} = 5$ Hz spectrum, and the cross-peaks from the two-bond correlations will be more intense in the $^{n}J_{CSi} = 5$ Hz spectrum than in the $^{n}J_{CSi} = 13$ Hz spectrum.

3D NMR of Addition Products 1 and 2. The f_1f_3 slices at $\delta_{^{29}Si} = -44.97$ from both the one-bond (Figure 4a) and multiple-bond (Figures 4b and 4c) 3D NMR spectra give well-resolved peaks for all the $^{1}H-^{13}C$ correlations that are attributed to **1**. They show CH_n group correlations related to Si_{IV} at $\delta_{^{29}Si} = -44.97$. Figure 4a contains a single cross-peak, which comes from the $^{1}H-^{13}C$ correlation of methine C(4)H one bond away from Si_{IV} of **1**. In addition to the resonances shown in Figure 4a, Figures 4b and 4c contain two additional pairs of resonances that are attributed to the $^{1}H-^{13}C$ correlations of methylenes $C(3)H_2/C(5)H_2$ and $C(2)H_2/C(6)H_2$ two and three bonds away from Si_{IV} atom of **1**, respectively. The cross-peak intensity differences in Figures 4b and 4c are not very large for this isomer. Most likely, this is because this isomer has both axial and equatorial substituents on the cyclohexyl ring and it is in rapid equilibrium between two chair conformers. One of these conformers will have a *trans* arrangement of Si_{IV} relative to the vicinal carbons, leading to a large $^{3}J_{CsSi}$, and the other will have a *gauche* arrangement of Si_{IV} relative to the vicinal carbons, leading to a small $^{3}J_{CSi}$. The average $^{3}J_{CSi}$ couplings in this structure will be reduced. In isomers with two equatorial cyclohexyl ring substituents the conformer with a *trans* arrangement of Si_{IV} relative to the vicinal carbons will be populated, resulting in larger $^{3}J_{CSi}$ couplings and larger

Table 1. Chemical Shift Assignments of Isomeric Compounds in Mixture (ppm)

	isomers					
atoms	**1**	**2**	**3**	**4**	**5**	**6**
^{29}Si(1)	−44.97(IV)	−45.97(II)	−44.69(V)	−45.94(I)	−44.65(VI)	−45.00(III)
^{29}Si(2)	−41.40(IV′)	−41.35(II′)	−41.45(V′)	−41.40(I′)	−41.07(VI′)	−41.23(III′)
^{1}H(1)	1.33	1.12	1.46	1.09	1.49	1.35
^{13}C(1)	38.62	40.74	36.95	41.72	40.76	40.28
^{1}H(2)	1.32/1.55	0.80/1.80	1.33/1.72	0.84/1.81	1.37	0.63
^{13}C(2)	31.00	34.33	31.55	33.14	27.39	28.03
^{1}H(3)	1.46/1.70	1.27/1.81	1.13	0.81	1.44/1.77	1.28/1.83
^{13}C(3)	24.16	27.02	17.84	22.66	25.80	27.55
^{1}H(4)	1.03	0.72	1.37	1.21/1.73	1.45/1.53	1.14/1.69
^{13}C(4)	21.15	22.78	27.03	27.00	26.91	27.90
^{1}H(5)	1.46/1.70	1.27/1.81	1.46	1.22/1.76	1.26/1.54	1.24/1.73
^{13}C(5)	24.16	27.00	23.30	28.09	24.52	26.66
^{1}H(6)	1.32/1.55	0.80/1.80	1.26/1.60	0.83/1.78	1.48/1.56	0.86/1.82
^{13}C(6)	31.00	34.33	31.60	33.25	30.03	32.59
^{1}H(7)	1.37	1.26	1.37	1.26	1.50/1.75	1.24/1.78
^{13}C(7)	27.32	30.66	27.04	30.60	26.19	28.97
^{1}H(8)	0.57	0.57	0.57	0.57	0.57	0.57
^{13}C(8)	6.94	6.37	7.01	6.52	7.79	6.03

differences between the cross-peak intensities in the 3D NMR spectra (see below).

The f_1f_3 slices at $\delta^{29}_{Si} = -45.57$ from both the one-bond (Figure 4d) and multiple-bond (Figures 4e and 4f) spectra contain well-resolved peaks for all the ^{1}H−^{13}C correlations that are attributed to **2**. They show correlations from CH_n groups related to the Si_{II} atom at $\delta^{29}_{Si} = -45.57$. Figure 4d shows a single resonance, which comes from the ^{1}H−^{13}C correlation of methine C(4)H one bond away from Si_{II} of **2**. In addition to the resonances found in Figure 4d, there are two pairs of resonances in Figures 4e and 4f. These resonances are attributed to the ^{1}H−^{13}C correlations of methylenes $C(3)H_2/C(5)H_2$ and $C(2)H_2/C(6)H_2$, which are two and three bonds away from Si_{II} of **2**, respectively. Although these two pairs of methylene resonances are similar to the patterns seen in Figures 4a, 4b, and 4c, the ^{1}H chemical shift differences for the geminal methylene resonances of **2** are much greater than those for the corresponding sets of resonances from **1**. This can be explained if **2** is the *trans*-substituted cyclohexane and **1** is the *cis*-isomer. In the *trans* isomer the molecule will primarily populate a conformation with both substituents in the equatorial positions, producing the maximum chemical shift differences for axial and equatorial geminal methylene protons on $C(3)H_2/C(5)H_2$ and $C(2)H_2/C(6)H_2$. Note the intensities of the cross-peaks in Figures 4e and 4f are significant and have the expected behavior.

In the *cis* isomer, both substituents cannot simultaneously populate the equatorial positions. Each of the two possible chair conformations must contain one axial substituent, raising their ground state energies and resulting in rapid ring flips between two similarly populated chair conformations possible. Therefore, the geminal methylene protons on $C(3)H_2/C(5)H_2$ and $C(2)H_2/C(6)H_2$ will exhibit shifts that are the population weighted averages of their shifts in the axial and equatorial positions. Because of the differences in the sizes of the $-Si(OMe)_3$ and $-CH_2CH_2Si(OMe)_3$ groups, the $-Si(OMe)_3$ substituent will preferentially populate the equatorial position in the *cis* isomer **1**. Therefore, the geminal methylene protons of the *cis* isomer should exhibit shifts that lie somewhere between the shifts of the corresponding protons in the *trans* isomer. This is in fact what is observed if the spectra in Figures 4b and 4c are compared with the spectra in Figures 4e and 4f. A situation might exist where four sets of resonances are observed for two geminal methylene protons (each in axial and equatorial positions if the ring flip were slow compared to the chemical shift difference, slow exchange). Alternatively, two sets of exchange-broadened resonances might exist which might be difficult to detect (if ring flipping occurred at a rate comparable to the shift difference, intermediate exchange).

3D NMR of Addition Products 3 and 4. The f_1f_3 slices at $\delta^{29}_{Si} = -44.69$ from both the one-bond (Figure 5a) and multiple-bond (Figures 5b and 5c) 3D NMR spectra give well-resolved peaks for all the ^{1}H−^{13}C correlations that are attributed to isomer **3**. It shows correlations from CH_n groups that are part of the structure containing Si_V at $\delta^{29}_{Si} = -44.69$. Figure 5a shows a single resonance, which comes from the ^{1}H−^{13}C correlation of the methine C(3)H, one bond away from Si_V of **3**. In Figures 5b and 5c, in addition to the resonance shown in Figure 5a, there are correlations from a single pair of nonequivalent geminal methylene resonances which are attributed to the ^{1}H−^{13}C correlations of methylene $C(2)H_2$. It is concluded that this group is two bonds away from Si_V, because this cross-peak is more intense in Figure 5c, the spectrum obtained with delays that were optimized for $^{n}J_{CSi} = 5$ Hz. Additionally, there are correlations from a methine C(1)H and several methylene $C(4)H_2$ and $C(5)H_2$ groups, two and three bonds away from Si_V of **3**. Ring flipping in this isomer falls in the fast exchange region, and the isomer significantly populates the two conformers, because chemical shift differences are not resolved for most of the geminal methylene protons.

The f_1f_3 slices at $\delta^{29}_{Si} = -45.94$ from both the one-bond (Figure 5d) and multiple-bond (Figures 5e and 5f) 3D NMR spectra give well-resolved peaks for all the ^{1}H−^{13}C correlations that are attributed to isomer **4**. It shows CH_n groups that are part of the structure containing the Si_I atom at $\delta^{29}_{Si} = -45.94$. Figure 5d shows a single resonance that comes from the ^{1}H−^{13}C correlation of methine C(3)H, one bond away from Si_I of **4**.

As compared to Figure 5d, there is an additional single resonance in Figure 5e from the ^{1}H−^{13}C correla-

tion of the methine C(1)H three bonds away from Si_I of **4**. In Figure 5e, there is also one pair of resonances from the $^1H-^{13}C$ correlation of the methylene C(5)H_2 three bonds away from the Si_I atom and a weak set of correlations from the methylene C(2)H_2 two bonds away from the Si_I. When compared to Figure 5e, Figure 5f contains additional pairs of resonances that are attributed to the $^1H-^{13}C$ correlation of methylenes C(2)H_2 and C(4)H_2 two bonds away from Si_I of **4** and a single resonance from the $^1H-^{13}C$ correlation of the side-chain methylene C(7)H_2 four bonds away from Si_I of **4**. The latter long-range four-bond coupling is not commonly resolved; however, in this isomer the atoms are locked in a W orientation, making such long-range couplings probable.

The relative configurations (i.e., *trans* or *cis*) of **3** and **4** are assigned using the same arguments described above for **1** and **2**. Note that only the methylene C(2)H_2 exhibits separate resonances for the geminal protons of **3** in Figures 5b and 5c. This is consistent with the fact that the geminal methylene protons of C(2)H_2 in **4** exhibit the largest chemical shift difference of all the methylene proton resonances. If ring flipping occurs in the intermediate exchange region, these resonances would require the fastest exchange rate to be averaged.

3D NMR of Addition Products 5 and 6. The f_1f_3 slices at $\delta_{^{29}Si} = -44.65$ from both the one-bond (Figure 6a) and multiple-bond (Figures 6b and 6c) 3D NMR spectra give well-resolved peaks for all the $^1H-^{13}C$ correlations that are attributed to isomer **5**. It shows correlations from CH_n groups that are part of the structure containing Si_{VI} at $\delta_{^{29}Si} = -44.65$. Figure 6a shows one resonance, which comes from the $^1H-^{13}C$ correlation of the methine C(2)H_2, one bond away from Si_{VI} of **5**. In addition to the resonance observed in Figure 6a, Figure 6b contains two additional pairs of resonances which are attributed to the $^1H-^{13}C$ correlation of methylenes C(4)H_2 and C(6)H_2, three bonds away from Si_{VI} of **5**, respectively. Additional correlations are not observed in Figure 6c; this is most likely because ring flipping occurs at a rate such that the remaining resonances are exchange broadened. It was not possible to vary the exchange rate to test this idea because the triple resonance probe needed to perform these 3D NMR experiments is limited to operation around room temperature, and resonances in this region of the spectrum are not resolved in the 1D or 2D NMR spectra.

The f_1f_3 slices at $\delta_{^{29}Si} = -45.00$ from both the one-bond (Figure 6d) and multiple-bond (Figures 6e and 6f) 3D NMR spectra give well-resolved peaks for all the $^1H-^{13}C$ correlations that are attributed to isomer **6**. They show correlations from CH_n groups that are part of the structure containing Si_{III} at $\delta_{^{29}Si} = -45.00$. Figure 6d shows one resonance, which comes from the $^1H-^{13}C$ correlation of the methine C(2)H, one bond away from the Si_{III} atom of **6**. In addition to the resonance shown in Figure 6d, Figure 6e contains two additional pairs of resonances which are attributed to the $^1H-^{13}C$ correlations of methylenes C(4)H_2 and C(6)H_2, three bonds away from Si_{III} of **6**. Figure 6f contains a new pair of resonances from the $^1H-^{13}C$ correlations of methylene C(3)H_2, two bonds away from Si_{III} of **6**, and another weak pair resonances due to $^1H-^{13}C$ correlation of methylene C(7)H_2, three bonds away from Si_{III} of **6**. Here the chemical shifts of the protons on the C(7)H_2 group are not identical because of the adjacent chiral center. Figure 6f also shows a single resonance that comes from the $^1H-^{13}C$ correlation of methine C(1)H, two bonds away from the Si_{III} atom of **6**. The additional pair of methylene cross-peaks result from bleed through of intense cross-peaks in adjacent slices.

Combining the data from 1D, 2D, and 3D NMR experiments, it is possible to resolve and assign all of the ^1H, ^{13}C, and ^{29}Si resonances of the six-isomer mixture **1**−**6** unambiguously. These chemical shift assignments are summarized in Table 1. Unambiguous structure proofs of all six components in the mixture have been achieved from NMR data alone, without resorting to physical separation of the individual isomers.

Conclusion

Triple resonance $^1H/^{13}C/^{29}Si$ 3D NMR techniques similar to those used in structural biology can be enormously useful for characterizing mixtures of isomeric structures. Applications of such techniques are possible, even when the isomeric structures contain low natural abundance nuclei such as ^{13}C and ^{29}Si studied in these mixtures. The resonance assignments obtained from this work can now serve as a basis for studying the kinetics and thermodynamics of hydrosilylation of these and related olefins.

Three-dimensional chemical shift correlation experiments provide enormous spectral dispersion and unique correlation of three coupled nuclei, when coherence from the right combination of nuclei is chosen. It is possible to provide resolved ^1H and ^{13}C correlation information based on the well-resolved ^{29}Si chemical shifts of the isomers. Similar applications of these experiments can be extremely useful in organometallic chemistry when the compounds contain a third NMR-active nucleus which exhibits resolvable *J*-coupling to ^{13}C (e.g., ^{119}Sn, ^{109}Ag, ^{103}Rh, ^{31}P, ^{19}F, etc.).

Acknowledgment. We wish to acknowledge the National Science Foundation (DMR-9617477 and DMR-0073346) for support of this research, and the Kresge Foundation and donors to the Kresge Challenge program at the University of Akron for funds used to purchase the 600 MHz NMR instrument used in this work.

Supporting Information Available: Six plots of 2D data from an INADEQUATE[23] NMR experiment performed on the mixture of **1**−**6** are presented which support the results from $^1H/^{13}C/^{29}Si$ 3D NMR experiment. The INADEQUATE NMR spectra are labeled to highlight the features that confirm the ^{13}C resonance assignments for each of the six structures in the mixture. This material is available free of charge via the Internet at http://pubs.acs.org.

OM020177X

(23) Bax, A.; Freeman, R.; Kempsell, S. P. *J. Am. Chem. Soc.* **1980**, *102*, 4851.
(24) Keeler, J.; Neuhaus, D. *J. Magn. Reson.* **1985**, *63*, 454.